

# Troponate/Aminotroponate Ruthenium–Arene Complexes: Synthesis, Structure, and Ligand-Tuned Mechanistic Pathway for Direct C–H Bond Arylation with Aryl Chlorides in Water

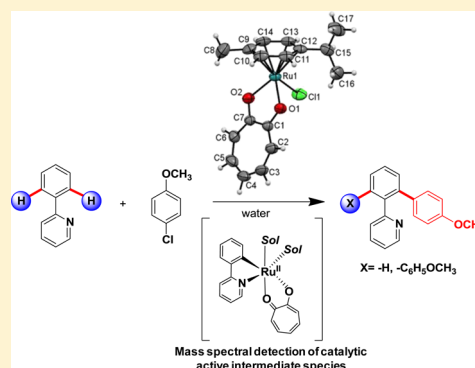
Ambikesh D. Dwivedi,<sup>†</sup> Chinky Binnani,<sup>†</sup> Deepika Tyagi,<sup>†</sup> Kuber S. Rawat,<sup>†</sup> Pei-Zhou Li,<sup>‡</sup> Yanli Zhao,<sup>‡</sup> Shaikh M. Mobin,<sup>†</sup> Biswarup Pathak,<sup>†,§</sup> and Sanjay K. Singh<sup>\*,†,§</sup>

<sup>†</sup>Discipline of Chemistry, School of Basic Sciences and <sup>§</sup>Centre for Material Science and Engineering, Indian Institute of Technology Indore, Indore 453552, Madhya Pradesh, India

<sup>‡</sup>Division of Chemistry and Biological Chemistry, School of Physical and Mathematical Sciences, Nanyang Technological University, 21 Nanyang Link 637371, Singapore

## Supporting Information

**ABSTRACT:** A series of water-soluble troponate/aminotroponate ruthenium(II)–arene complexes were synthesized, where O,O and N,O chelating troponate/aminotroponate ligands stabilized the *piano-stool* mononuclear ruthenium–arene complexes. Structural identities for two of the representing complexes were also established by single-crystal X-ray diffraction studies. These newly synthesized troponate/aminotroponate ruthenium–arene complexes enable efficient C–H bond arylation of arylpyridine in water. The unique structure–activity relationship in these complexes is the key to achieve efficient direct C–H bond arylation of arylpyridine. Moreover, the steric bulkiness of the carboxylate additives systematically directs the selectivity toward mono- versus diarylation of arylpyridines. Detailed mechanistic studies were performed using mass-spectral studies including identification of several key cyclometalated intermediates. These studies provided strong support for an initial cycloruthenation driven by carbonate-assisted deprotonation of 2-phenylpyridine, where the relative strength of  $\eta^6$ -arene and the troponate/aminotroponate ligand drives the formation of cyclometalated 2-phenylpyridine Ru–arene species,  $[(\eta^6\text{-arene})\text{Ru}(\kappa^2\text{-C,N-phenylpyridine})(\text{OH}_2)]^+$  by elimination of troponate/aminotroponate ligands and retaining  $\eta^6$ -arene, while cyclometalated 2-phenylpyridine Ru–troponate/aminotroponate species  $[(\kappa^2\text{-troponate/aminotroponate})\text{Ru}(\kappa^2\text{-C,N-phenylpyridine})(\text{OH}_2)_2]$  was generated by decoordination of  $\eta^6$ -arene ring during initial C–H bond activation of 2-phenylpyridine. Along with the experimental mass-spectral evidence, density functional theory calculation also supports the formation of such species for these complexes. Subsequently, these cycloruthenated products activate aryl chloride by facile oxidative addition to generate C–H arylated products.



## INTRODUCTION

Chemistry of ruthenium(II)–arene-based complexes has been established as a promising field of organometallic chemistry because of the structural versatility and unique tunable structure–activity behavior shown by these complexes. Therefore, these complexes are being used as important candidates as catalysts in a wide range of organic transformations, biological applications such as active water-soluble antitumor agents, and so on.<sup>1–3</sup> Careful observation of the scientific progress in the field of arene–ruthenium complexes revealed that the most active class of these complexes contains nitrogen or oxygen donor ligands.<sup>1,2</sup>

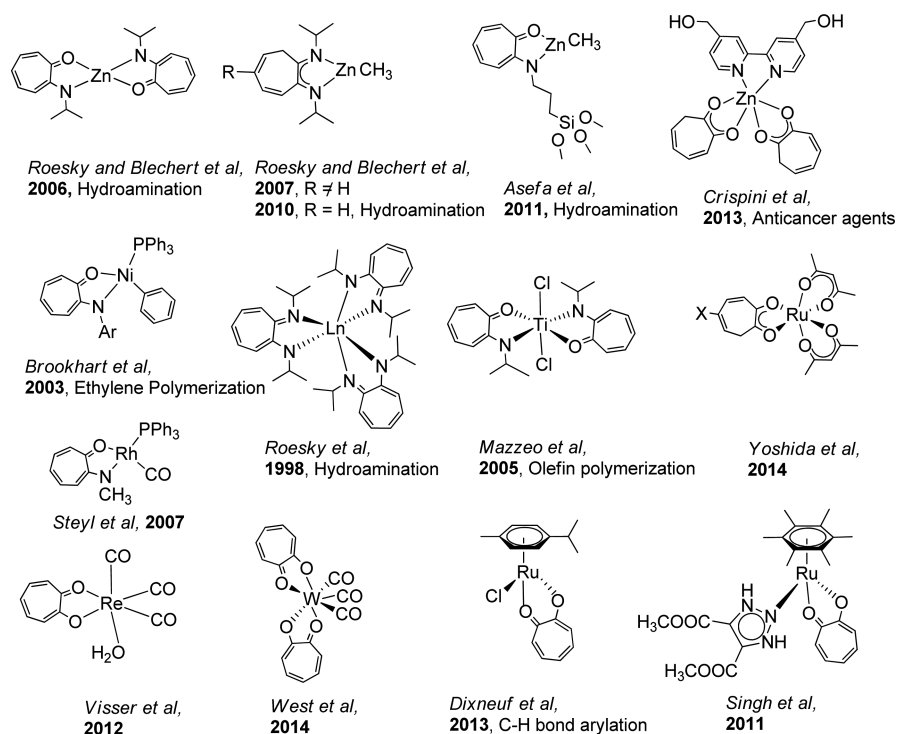
In this context, chemistry of tropolone and 2-aminotropones has been extensively explored in recent past for several applications, such as anticancer agent<sup>4</sup> and as active catalyst for various important reactions such as intramolecular hydroamination,<sup>5–7</sup> ethylene polymerization,<sup>8</sup> olefin polymerization,<sup>9</sup> and so on<sup>10–14</sup> (shown in Scheme 1). Tropolone-based complexes have several unique features such as (i) the formation of strained five-membered chelating ring with the metal center, (ii) have enolic

hydroxy group analogous to  $\beta$ -diketone, and (iii) negative charge accumulation predominantly on nitrogen atoms of aminotroponate ligands. Moreover, the planar large seven-membered homoaromatic rings of tropolone or aminotropones substantially contribute in the stability of these complexes.

In recent years, remarkable progress has been accomplished in C–H bond activation as a direct route for C–C bond formation reactions.<sup>1a,15</sup> Several other metals such as Pd,<sup>16</sup> Rh,<sup>17</sup> and Ir<sup>18</sup> based complexes were also explored for C–H bond activation, but ruthenium complexes, being relatively less expensive, non-toxic, and stable in air and water, gained advantages over others.<sup>12</sup> Among the most efficient ruthenium catalysts investigated so far for C–H bond activation or functionalization, ruthenium–arene complexes such as  $[(\eta^6\text{-arene})\text{RuCl}_2]_2$  or its carboxylate complexes represent the highly active class of catalysts.<sup>19</sup> However, other ruthenium complexes such as those containing or involving

Received: April 25, 2016

Scheme 1. Troponone and Aminotroponone-based Metal Complexes



phosphine ligands and others like  $\text{RuCl}_2(\text{PPh}_3)_3$ ,  $[\text{RuCl}_2(\text{cod})]_2$ , and  $[(\eta^6\text{-arene})\text{RuCl}_2(1,2\text{-diphenylvinyl})\text{phosphine}]$  as well as  $[\{(\eta^6\text{-arene})\text{RuCl}_2\}_2]$  with excess of  $\text{PPh}_3$  were also explored, but those are expected to follow a different reaction pathway.<sup>20</sup> Most of these reactions were performed in organic solvents, such as *N*-methyl-2-pyrrolidone (NMP) or toluene, but recently huge efforts have been devoted to develop efficient catalytic systems for C–H bond activation in more environmentally tolerant solvents such as diethylcarbonate or water.<sup>21</sup>

Analogous to carboxylate ligands, ruthenium–arene complexes containing several other O,O or N,O chelating ligands for C–H bond activation were also reported in water, where diarylation is favored with N,O chelating ligands, but phosphine-containing complexes showed poor catalytic activity.<sup>22</sup> Similarly,  $\beta$ -ketonates-based ruthenium–arene complexes have also been employed for C–H bond arylation in NMP, where sterically bulky diketonate favors monoarylation.<sup>23</sup> Unlike weakly coordinating carboxylate ligands, these strongly chelating O,O or O,N ligands displayed high affinity toward metal center, and therefore we anticipated that presumably ruthenium–arene complexes containing such strongly coordinating chelating ligands might follow a different catalytic reaction pathway or involve different catalytically active species during C–H bond activation, in contrast to the well-established carboxylate/carbonate-driven cycloruthenated species,  $[(\eta^6\text{-arene})\text{Ru}(\kappa^2\text{-C},\text{N}\text{-phenylpyridine})(\text{sol})]^+$  observed with ruthenium–arene complexes.

Herein, we report the synthesis and characterization of eight novel ruthenium–arene complexes, **[Ru]-1**–**[Ru]-8**, containing troponate (**L1**) and substituted aminotroponate (isopropylaminotroponate (**L2**) and cyclohexylaminotroponate (**L3**)) ligands. Structures of the ligand **L3** and two of the representative ruthenium–arene complexes  $[(\eta^6\text{-}p\text{-cymene})\text{Ru}(\kappa^2\text{-O},\text{O}\text{-troponate})\text{Cl}]$  (**[Ru]-1**) and  $[(\eta^6\text{-}p\text{-cymene})\text{Ru}(\kappa^2\text{-O},\text{N}\text{-isopropylaminotroponate})\text{Cl}]$  (**[Ru]-3**) were authenticated by single-crystal X-ray diffraction studies. Further, these complexes were employed for ortho C–H bond

arylation of 2-phenylpyridine with 4-chloroanisole in water. Effect of several carboxylate additives and structural motifs of troponate/aminotroponate ruthenium–arene complexes on catalytic activity and selectivity toward C–H bond mono vs diarylation were explored. Main focus of the present report is to extensively investigate, identify, and characterize catalytically active species and/or reaction intermediates of the C–H bond arylation as catalyzed by newly synthesized troponate/aminotroponate ruthenium–arene complexes using mass-spectral and  $^1\text{H}$  NMR studies. On the basis of these studies, along with the support from density functional theory (DFT) calculation, the catalytic reaction pathway was proposed.

## RESULTS AND DISCUSSION

**Synthesis and Characterization of Troponate-/Aminotroponate Ruthenium(II)–Arene Complexes.** Troponate/aminotroponate ruthenium(II)–arene complexes were synthesized by reacting troponone (**L1**), 2-(isopropylamino)troponone (**L2**), or 2-(cyclohexylamino)troponone (**L3**) ligands with ruthenium–arene precursors. Aminotroponone-based ligands **L2** and **L3** were prepared by direct nucleophilic displacement of the tosyl group of the 2-(tosyloxy)troponone by using excess of corresponding amine (isopropylamine or cyclohexylamine) applying an earlier reported method.<sup>6</sup> The synthesized ligands were characterized by several spectro-analytical techniques, which confirmed the proposed structures (see the [Experimental Section](#)). Structural characterization of the ligand **L3** was also elucidated by single-crystal X-ray diffraction of its suitable crystals obtained by slow evaporation of hexane–ethyl acetate (98:2, v/v) at room temperature. ORTEP diagram of the ligand **L3** is shown in [Figure 1](#). Crystallographic data and bond parameters for **L3** are listed in [Tables S1](#) and [S2](#). The C–O and C–N bond lengths (1.2478(18) and 1.3317(19) Å, respectively) are of intermediate value for single and double bonds, which is similar to reported aminotroponone ligand.<sup>8</sup>

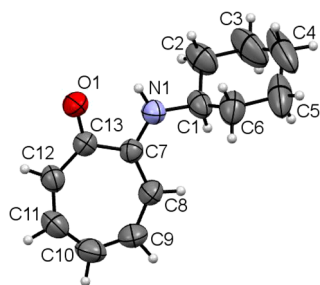


**Figure 1.** Single-crystal X-ray structure of 2-(cyclohexylamino)tropolone (**L3**). Selected bond lengths (Å): C13–O1 = 1.2478(18), C7–N1 = 1.3317(19), C1–N1 = 1.4548(19), bond angles (deg): C7–C13–O1 = 116.37(13), C13–C7–N1 = 111.27(12) and torsion angles (deg): O1–C13–C7–N1 = –4.5(2), C8–C7–C13–O1 = 174.1(2), C12–C13–C7–N1 = 174.6(1).

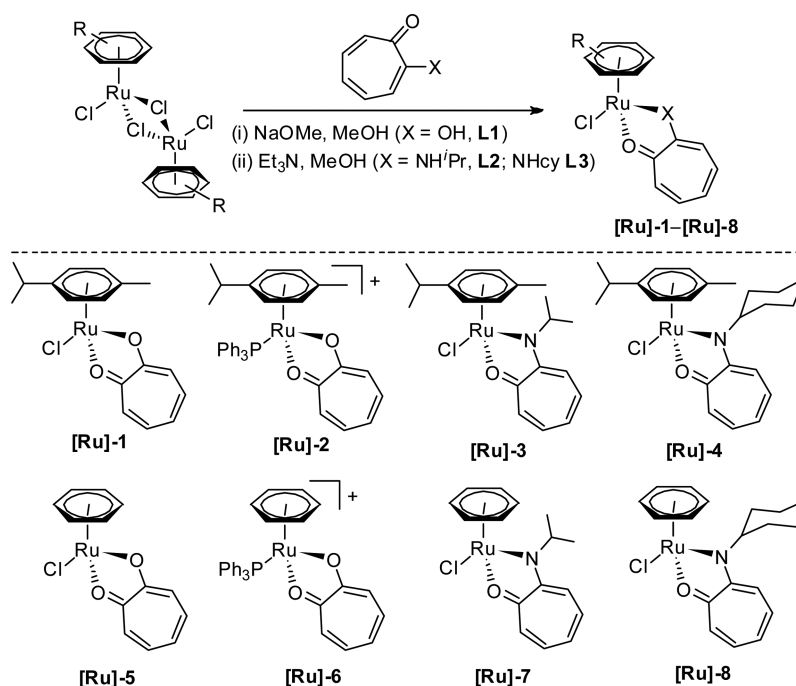
Tropolone (**L1**) or aminotropolone (**L2** and **L3**) ligands were reacted with ruthenium–arene precursors,  $[\{(\eta^6\text{-arene})\text{RuCl}_2\}_2]$  ( $\eta^6\text{-arene} = \eta^6\text{-C}_{10}\text{H}_{14}$  and  $\eta^6\text{-C}_6\text{H}_6$ ) in methanol using a base (or without base) to afford water-soluble mononuclear *piano-stool* troponate/aminotroponate ruthenium(II)–arene complexes in good yield (Scheme 2). The synthesized complexes have the general formula of  $[(\eta^6\text{-arene})\text{Ru}(\kappa^2\text{-L})\text{Cl}]$  (L = **L1**,  $\eta^6\text{-arene} = \eta^6\text{-C}_{10}\text{H}_{14}$  (**[Ru]-1**) and  $\eta^6\text{-C}_6\text{H}_6$  (**[Ru]-5**); L = **L2**,  $\eta^6\text{-arene} = \eta^6\text{-C}_{10}\text{H}_{14}$  (**[Ru]-3**) and  $\eta^6\text{-C}_6\text{H}_6$  (**[Ru]-7**); L = **L3**,  $\eta^6\text{-arene} = \eta^6\text{-C}_{10}\text{H}_{14}$  (**[Ru]-4**) and  $\eta^6\text{-C}_6\text{H}_6$  (**[Ru]-8**) and  $[\{(\eta^6\text{-arene})\text{Ru}(\kappa^2\text{-L1})(\text{PPh}_3)\}_2]^+$  ( $\eta^6\text{-arene} = \eta^6\text{-C}_{10}\text{H}_{14}$  (**[Ru]-2**) and  $\eta^6\text{-C}_6\text{H}_6$  (**[Ru]-6**)). The spectro-analytical analyses of the synthesized complexes corroborated well with the proposed structures (see the Experimental Section).

In the  $^1\text{H}$  NMR spectra of the mononuclear complex **[Ru]-1**–**[Ru]-8**, arene protons displayed downfield shift as compared to that in the respective precursor ruthenium–arene dimer. Moreover, ring carbon of the coordinated tropolone in complexes **[Ru]-1** and **[Ru]-5** also resonated in slightly deshielded region (126.34–137.80 ppm) compared to that of the free tropolone

ligand. However, the carbonyl carbons, in particular, of the tropolone ligand in complexes **[Ru]-1** and **[Ru]-5** resonated in more deshielded region at 184.29–184.87 ppm compared to that for free tropolone ligand (171.84 ppm), suggesting the coordination of the ligand to the metal center. The conjugative and electron-donating abilities of the troponate/aminotroponate ligands decreases electron density that troponate/aminotroponate ring might have contributed in the observed downfield shift in the  $^1\text{H}$  and  $^{13}\text{C}$  NMR spectra.<sup>24</sup> In agreement with the NMR results, Fourier transform infrared (FTIR) spectra of the complexes **[Ru]-1** and **[Ru]-5** show a typical band at 1588.21 and 1588.38  $\text{cm}^{-1}$ , respectively, for the  $\nu(\text{C}=\text{O})$ , while it appeared at 1609  $\text{cm}^{-1}$  in the free tropolone ligand, suggesting the lengthening of  $\text{C}=\text{O}$  bonds upon coordination of tropolone to metal center.<sup>25,26</sup> Cyclic voltammograms of the representative complexes **[Ru]-1** and **[Ru]-5** were obtained in  $\text{CH}_2\text{Cl}_2$  containing 0.1 M (*n*-Bu<sub>4</sub>N)PF<sub>6</sub> as supporting electrolyte at a sweep rate of 50 mV/s at room temperature (Figures S1 and S2). On the one hand, in the anodic window (0 to +2.0 mV) of cyclic voltammogram for complexes **[Ru]-1** and **[Ru]-5**, a well-defined quasi-reversible oxidation reduction wave was observed at 0.939 and 1.023 mV, respectively,<sup>27</sup> which may be attributed to  $\text{Ru}^{\text{II/III}}$  redox couple. Analogously for the aminotroponate ruthenium–arene complex **[Ru]-2**, the  $\text{Ru}^{\text{II/III}}$  redox couple appeared at 1.173 mV. On the other hand, tropolone-based reduction waves appeared in the cathodic potential window (0 to –2.0 mV) of cyclic voltammogram of these complexes (Table S4). Methyl substitution at arene ligand in complex **[Ru]-1** resulted in a shift of  $\text{Ru}^{\text{II/III}}$  redox couple toward less positive side, due to the increase in electron density on the metal center, which destabilizes the ground-state energy and therefore leads to a lowering of the metal-based oxidation potentials.<sup>28</sup>

X-ray suitable crystals of complexes **[Ru]-1** and **[Ru]-3** were obtained by slow evaporation method using dichloromethane and diethyl ether as solvents, and their molecular structures were confirmed by single-crystal X-ray diffraction analysis.

**Scheme 2.** Synthesis of Ruthenium(II)–Arene Complexes Containing Tropolone-based Ligands



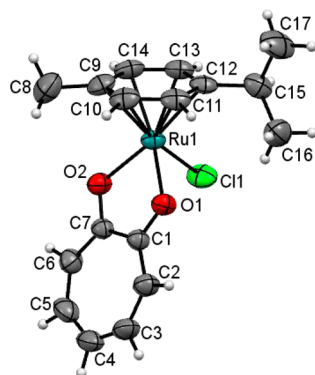


**Figure 2.** Single-crystal X-ray structure of troponate ruthenium(II) *p*-cymene complex ([**Ru**]-1). Selected bond lengths (Å): Ru1–C<sub>avg</sub> = 2.167, Ru1–C<sub>ct</sub> = 1.645, Ru1–Cl1 = 2.4094(8), Ru1–O1 = 2.0789(18), Ru1–O2 = 2.079(2), C1–O1 = 1.284(3), C7–O2 = 1.289(3), bond angles (deg): O1–Ru1–O2 = 76.63(7), O1–Ru1–Cl1 = 84.48(6), O2–Ru1–Cl1 = 84.47(6) and torsion angle (deg): O1–C1–C7–O2 = –1.5(4).

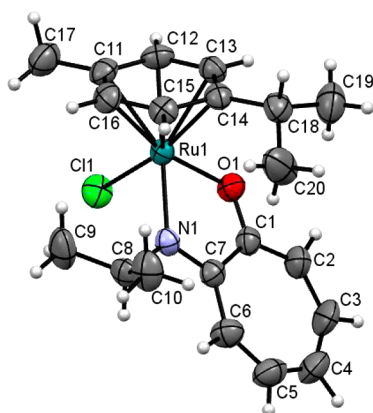


**Figure 3.** Single-crystal X-ray structure of isopropylaminotroponate–ruthenium(II) *p*-cymene complex ([**Ru**]-3). Selected bond lengths (Å): Ru1–C<sub>avg</sub> = 2.188, Ru1–C<sub>ct</sub> = 1.676, Ru1–Cl1 = 2.4196(8), Ru1–O1 = 2.0463(19), Ru1–N1 = 2.115(3), C1–O1 = 1.277(4), C7–N1 = 1.319(4), bond angles (deg): C1–Ru1–N1 = 84.68(7), O1–Ru1–Cl1 = 85.93(6), O1–Ru1–N1 = 75.86(9) and torsion angle (deg): O1–C1–C7–N1 = 0.5(4).

The ORTEP view along with the selected bond parameters of the complexes [**Ru**]-1 and [**Ru**]-3 are shown in Figures 2 and 3, respectively. Crystallographic data and bond parameters of these complexes are listed in Table 1 and Table S3, respectively. Both the complexes adopted the *piano-stool* geometry, where the  $\eta^6$ -coordinated arene ring is present as top disc of stool, and two O atoms of the ligand L1 or N and O atoms of the ligand L3 along with one chloride ligand are as three legs of the stool. The complex [**Ru**]-1 crystallized in monoclinic crystal system with *P21/n* space group. The arene ring (in  $\eta^6$ -*p*-cymene) appears almost planar for both the complexes [**Ru**]-1 and [**Ru**]-3, where the displacements of the arene ring centroid from the Ru(II) center are 1.645 and 1.676 Å, respectively, for complexes [**Ru**]-1 and [**Ru**]-3. The Ru–C<sub>centroid</sub> and Ru–C bond distances are also comparable with other similar complexes.<sup>2,26</sup> The angle between the legs and the centroid of the  $\eta^6$ -arene ring (*C<sub>i</sub>*) are in the range of 129.63°–131.17°. Both the Ru–oxygen bond distances, 2.0789 Å (Ru1–O1) and 2.079 Å (Ru1–O2), are comparable for the coordinated tropolone in complex [**Ru**]-1.<sup>27</sup> Moreover, the comparable bond lengths of C1–O1 (1.284 Å) and C7–O2

**Table 1.** Crystal Data and Structure Refinement Details for [**Ru**]-1 and [**Ru**]-3

structure	complex [ <b>Ru</b> ]-1	complex [ <b>Ru</b> ]-3
empirical formula	C <sub>17</sub> H <sub>19</sub> ClO <sub>2</sub> Ru	C <sub>20</sub> H <sub>26</sub> ClNORu
Fw	391.84	432.94
<i>T</i> (K)	293(2)	293(2)
$\lambda$ (Å)	0.71073	0.71073
cryst system	monoclinic	monoclinic
space group	<i>P21/n</i>	<i>P21/c</i>
cryst size, mm ( <i>l</i> × <i>k</i> × <i>h</i> )	0.12 × 0.10 × 0.09	0.33 × 0.27 × 0.21
<i>a</i> , Å	10.6918(5)	14.7074(4)
<i>b</i> , Å	13.3978(6)	16.6899(3)
<i>c</i> , Å	11.4591(5)	7.7339(2)
$\alpha$ , deg	90.00	90.00
$\beta$ , deg	99.654(4)	102.751(2)
$\gamma$ , deg	90.00	90.00
<i>V</i> , Å <sup>3</sup>	1618.23(12)	1851.58(8)
<i>Z</i>	4	4
$\rho_{\text{calcd}}$ , g cm <sup>–3</sup>	1.608	1.553
$\mu$ , mm <sup>–1</sup>	1.135	0.997
<i>F</i> (000)	792	888
$\theta$ range, deg	3.24–29.84	3.535–24.994
completeness to $\theta_{\text{max}}$	83.2	99.8
no. of data collected/ unique data	7476/3856	14 307/3250
	[ <i>R</i> (int) = 0.0240]	[ <i>R</i> (int) = 0.0522]
params/restraints	193/0	222/0
goodness of fit on <i>F</i> <sup>2</sup>	1.043	1.100
final <i>R</i> indices [ <i>I</i> > 2 $\sigma$ ( <i>I</i> )]	<i>R</i> 1 = 0.0318 <i>wR</i> 2 = 0.0688	<i>R</i> 1 = 0.0297 <i>wR</i> 2 = 0.0728
<i>R</i> indices (all data)	<i>R</i> 1 = 0.0479 <i>wR</i> 2 = 0.0786	<i>R</i> 1 = 0.0350 <i>wR</i> 2 = 0.0782

(1.289 Å) are in complex [**Ru**]-1, suggesting a delocalization of the C=O bond of the tropolone ligand upon coordination.<sup>26</sup> The bite angle (O1–Ru1–O2) of the tropolone ligand in complex [**Ru**]-1 is 76.63°. The Cl1–Ru1–O1 and Cl1–Ru1–O2 bond angles are 84.48° and 84.47°, respectively, for complex [**Ru**]-1. The Ru1–O1 and Ru1–N1 bond lengths in complex [**Ru**]-3 are 2.0463 and 2.115 Å, respectively. The C–O (1.277 Å) bond length appears slightly shorter in complex [**Ru**]-3 than in the Ru–tropolone complex [**Ru**]-1. Moreover, the bite angle of the aminotroponate ligand in complex [**Ru**]-3 is 75.86°, which deviates only slightly from the bite angle of the parent complex [**Ru**]-1 with troponate ligand. Replacing one of the oxygen atoms in ligand L1 with nitrogen (in ligand L3) resulted in no significant distortion in the planarity of the tropolone backbone (torsion angle O1–C1–C7–N1 = 0.5(4)). For complex [**Ru**]-3, the Cl1–Ru1–O1 and Cl1–Ru1–N1 bond angles are 85.93° and 84.68°. Bond angle between the legs and the centroid of the  $\eta^6$ -arene ring (*C<sub>i</sub>*) is 129.63°–131.17° and 126.70°–136.67° in complexes [**Ru**]-1 and [**Ru**]-3, respectively.<sup>2,26</sup> The observed values are comparable to those reported for other analogous complexes.<sup>26,29</sup>

#### Arene–Ru(II) Catalyzed C–H Bond Arylation in Water.

At an outset of our investigations for C–H bond arylation, 2-phenylpyridine (0.5 mmol) was treated with 4-chloroanisole (1.25 mmol) in water in the presence of 5 mol % troponate Ru–*p*-cymene catalyst, [**Ru**]-1, and 3 equiv of K<sub>2</sub>CO<sub>3</sub> at 100 °C, without using any carboxylate additive. Results inferred that [**Ru**]-1 catalyst is reactive in water and facilitates C–H bond arylation even with aryl chlorides with 86% conversion of 2-phenylpyridine. The monoarylated to diarylated product selectivity was found to be

**Table 2.** Screening of Troponate-/Aminotroponate Ru–Arene Catalysts for C–H Bond Arylation Reaction in Water<sup>a</sup>

entry	catalysts	conv (%)	sel % (m/d) <sup>b</sup>	TON
1	$[(\eta^6\text{-}p\text{-cymene})\text{Ru}(\kappa^2\text{-}O,O\text{-troponate})\text{Cl}]$ ([Ru]-1)	86	61/39	17.2
2	$[(\eta^6\text{-}p\text{-cymene})\text{Ru}(\kappa^2\text{-}O,O\text{-troponate})\text{PPh}_3\text{Cl}]$ ([Ru]-2)	95	73/27	19.0
3	$[(\eta^6\text{-}p\text{-cymene})\text{Ru}(\kappa^2\text{-}N,O\text{-isopropylaminotroponate})\text{Cl}]$ ([Ru]-3)	75	82/18	15.0
4	$[(\eta^6\text{-}p\text{-cymene})\text{Ru}(\kappa^2\text{-}N,O\text{-cyclohexylaminotroponate})\text{Cl}]$ ([Ru]-4)	81	83/17	16.2
5	$[(\eta^6\text{-benzene})\text{Ru}(\kappa^2\text{-}O,O\text{-troponate})\text{Cl}]$ ([Ru]-5)	58	85/15	11.6
6	$[(\eta^6\text{-benzene})\text{Ru}(\kappa^2\text{-}O,O\text{-troponate})\text{PPh}_3\text{Cl}]$ ([Ru]-6)	90	80/20	18.0
7	$[(\eta^6\text{-benzene})\text{Ru}(\kappa^2\text{-}N,O\text{-isopropylaminotroponate})\text{Cl}]$ ([Ru]-7)	48	85/15	9.6

<sup>a</sup>Reaction conditions: 2-phenylpyridine (0.5 mmol), 4-chloroanisole (1.25 mmol), [Ru] catalyst (5 mol %),  $\text{K}_2\text{CO}_3$  (1.5 equiv), water (5 mL), 16 h. <sup>b</sup>Obtained from <sup>1</sup>H NMR.

61:39 (results are shown in Table 2). Notably, the [Ru]-1 catalyst exhibited high conversion even in the absence of carboxylate additives. Literature reports evidenced that carboxylates have a significant role as deprotonating agent during the C–H bond activation reactions catalyzed by transition-metal complexes.<sup>1a,30</sup> Therefore, as an attempt to investigate the role of carboxylate additives on the C–H bond arylation (conversion and selectivities for mono- and diarylated products), [Ru]-1 catalyst was treated with 2-phenylpyridine and 4-chloroanisole under analogous conditions as described above but with added potassium salts of carboxylates, starting from acetate to propionate, isobutyrate, and pivalate. Using acetate and its methyl-substituted analogues, we could be able to establish a relation between the steric bulkiness of additives and the selectivity of C–H bond arylated products (mono and diarylated). As depicted in Figure 4, with an increase

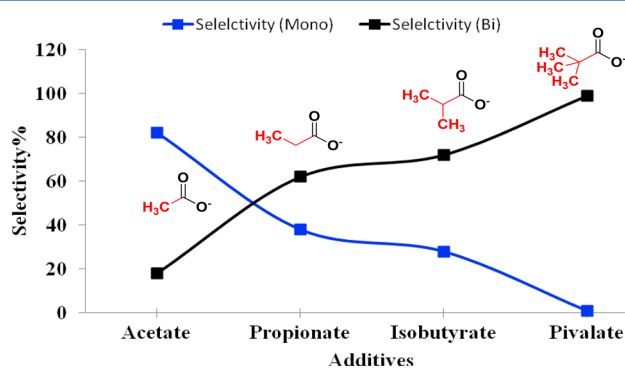


**Figure 4.** Effect of additives on the selectivity toward mono- vs di-C–H arylated products from the reaction of 2-phenylpyridine with 4-chloroanisole catalyzed by [Ru]-1 catalyst.

in the bulkiness of additives, the selectivity shifts toward diarylated product in the order of pivalate > isobutyrate > propionate > acetate. The selectivity for monoarylated product was 82% with acetate, which was further decreased to 38% and 28%, respectively, with potassium propionate and potassium isobutyrate. This trend persists even to bulkier potassium pivalate, where only 1% selectivity for monoarylated product (99% diarylation) was observed.

The observed behavior of carboxylate additives on the selectivity for C–H bond arylation is interesting and suggests the intriguing involvement of carboxylates in C–H bond

activation reaction pathway, as carboxylate can bind with metal center (such as acetate) or remains in the solution (such as pivalate) and therefore may be involved in intra/intermolecular deprotonation of 2-phenylpyridine.<sup>31,32</sup> To further investigate this phenomenon, we performed mass-spectral analysis of the reaction mixture obtained after 3 h of reaction of [Ru]-1 catalyst (0.025 mmol) with carboxylate (0.05 mmol) in the presence of  $\text{K}_2\text{CO}_3$  (1.5 mmol) at 100 °C in water under Ar atmosphere (Figure 5). Mass-spectral results showed that, along with the peaks of the [Ru]-1 catalyst at  $m/z$  357.33 ( $[\text{M}-\text{Cl}]^+$ ), acetate-coordinated species  $[(\eta^6\text{-arene})\text{Ru}(\kappa^2\text{-troponate})(\kappa^1\text{-acetate})] + \text{Na}^+$  at  $m/z$  439.28 was also observed with relative abundance of 37%. In contrast to the high abundance of acetate-coordinated species, abundance for analogous pivalate coordinated species,  $[(\eta^6\text{-arene})\text{Ru}(\kappa^2\text{-troponate})(\kappa^1\text{-pivalate})] + \text{CH}_3\text{CN} + 2\text{Na}^+$  at  $m/z$  547.07 was observed to be very low (12%). These results are consistent with earlier reports that acidity of pivalate increases in water, which destabilizes the Ru–pivalate bond and therefore results in the increment of free pivalate in the reaction mixture.<sup>21</sup> Moreover, increase in the steric bulkiness of these carboxylates, from acetate to pivalate, presumably also favors easy decoordination of bulky carboxylates. Interestingly, reaction with carboxylates does not lead the de-coordination of troponate ligand in [Ru]-1 catalyst, suggesting the stability of troponate Ru–arene species.

Further, to investigate and establish structure–activity relationship, [Ru]-1 to [Ru]-7, structural analogues of [Ru]-1 catalyst, were synthesized using different  $\eta^6$ -*p*-cymene/benzene and tropolone/aminotroponone ligands; catalytic efficiency of these complexes was evaluated for the direct C–H bond arylation of 2-phenylpyridine under the optimized reaction condition (Table 2). Results implied that Ru–*p*-cymene complexes [Ru]-1–[Ru]-4 (Table 2, entries 1–4) displayed high conversions of 2-phenylpyridine (75% to 95%); in contrast, Ru–benzene complexes (Table 2, entries 5–7) exhibited relatively low conversions (48% to 90%). Moreover, Ru–*p*-cymene complexes favor mono- to diarylated ( $m/d$ ) products ( $m/d$  61:39 [Ru]-1 and 73:27 [Ru]-2), more in comparison to Ru–benzene complexes,  $m/d$  85:15, [Ru]-5 and 80:20, [Ru]-6 (Table 2, entries 1, 2, 5, and 6). In contrast to troponate Ru–*p*-cymene complex [Ru]-1, a remarkable improvement in mono- to diarylated product ratio was observed with aminotroponate Ru–*p*-cymene complex, [Ru]-3 ( $m/d$  82:18) and [Ru]-4 ( $m/d$  83:17; Figure 6). However, the substitution at the N atom of the aminotroponate Ru–arene complexes has no distinct effect on mono- to diarylated ratio ( $m/d$ , *N*-isopropyl = 82:18, [Ru]-3 and *N*-cyclohexyl = 83:17, [Ru]-4 (Figure 6).

Further to elucidate the reaction mechanism, extensive mass spectrometric investigations were performed for the ruthenium-catalyzed C–H bond activation under the optimized reaction condition. As previously reported, ruthenium complexes are found to be very efficient to form cyclometalated intermediates by C–H activation at ortho position of the phenyl ring.<sup>33</sup> Stoichiometric reactions of 2-phenylpyridine and [Ru]-1 catalyst were performed in water in the presence of  $\text{K}_2\text{CO}_3$  (3 equiv) base at 100 °C in catalyst-to-substrate molar ratio of 1:1. After 3 h, reaction mixture was subjected to mass-spectral analysis, where several cycloruthenated 2-phenylpyridine species were identified. To our surprise, along with the well-established key intermediate cyclometalated species  $\{(\eta^6\text{-arene})\text{Ru}(\kappa^2\text{-}C,N\text{-phenylpyridine})\}^+$  [Ru]-A at  $m/z$  390.01, another cyclometalated species with troponate ligand at  $m/z$  379.13 corresponding to  $\{(\kappa^2\text{-troponate})\text{-Ru}(\kappa^2\text{-}C,N\text{-phenylpyridine})\}$  ([Ru]-B) was also observed, where tropolone ligand was retained instead of *p*-cymene ring.

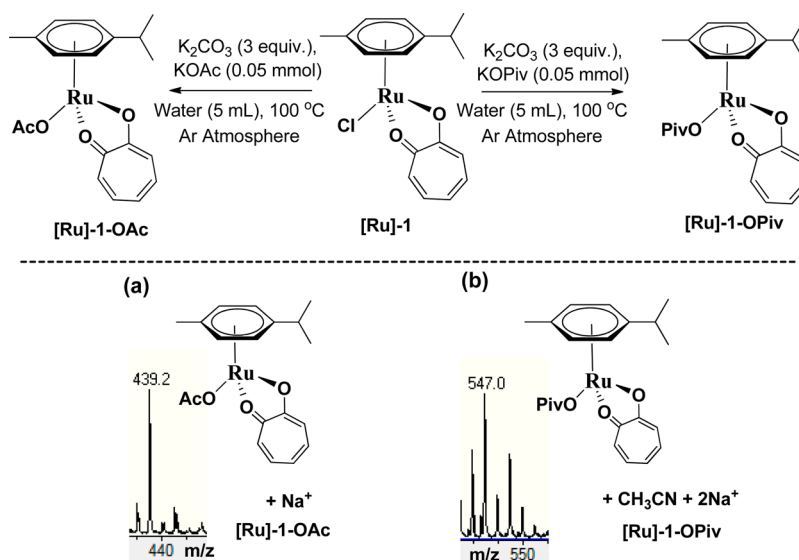


**Figure 5.** Mass-spectral analysis of the reaction of **[Ru]-1** catalyst with acetate and pivalate to identify (a)  $(\eta^6\text{-arene})\text{Ru}(\kappa^2\text{-troponate})(\kappa^1\text{-acetate}) + \text{Na}^+$  and (b)  $[(\eta^6\text{-arene})\text{Ru}(\kappa^2\text{-troponate})(\kappa^1\text{-pivalate})] + \text{CH}_3\text{CN} + 2\text{Na}^+$  species.

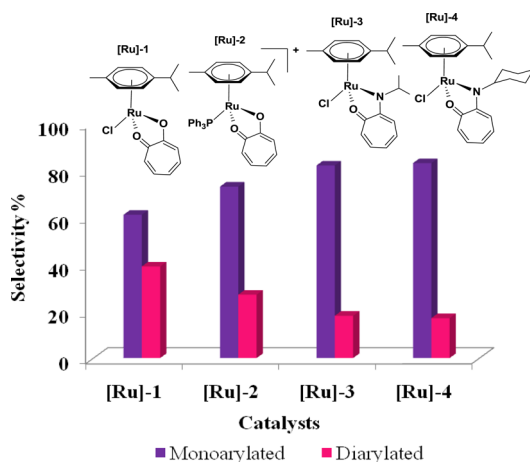


**Figure 6.** Effect of different Ru(II) catalysts on the selectivity of mono- vs di- C–H arylated products of 2-phenylpyridine.

Analogous reactions were conducted but with high substrate-to-catalyst (*S/C*) ratio of 2:1 or larger (5:1), which inferred that

there is more tendency of arene (*p*-cymene) cleavage to generate the **[Ru]-B** species. Mass spectra of the reaction mixture obtained from the reaction of **[Ru]-1** catalyst with 2-phenylpyridine at substrate/catalyst ratios of 1:1, 2:1, and 5:1 revealed that the relative percentages of the formation of **[Ru]-A** and **[Ru]-B** are 60:40, 42:58, and 16:84, respectively (Figure S3). To further investigate the relevance of this newly identified troponate Ru–cyclometalated species **[Ru]-B**, reaction mixture was analyzed by mass spectrometry with respect to reaction time. Notably, the mass-spectral analysis revealed a systematic enhancement in the abundance of the **[Ru]-B** species with time, whereas that of **[Ru]-A** species decreases (Figure 7). To further authenticate if analogous species were also generated with the troponate/aminotroponate Ru(II) complexes, we performed the mass-spectral analysis of the reaction of **[Ru]-3** catalyst with 2-phenylpyridine in substrate-to-catalyst ratio of 2:1 under analogous reaction conditions. Analogous to that observed with **[Ru]-1** catalyst, replacing troponate ligand with *N*-isopropyl–aminotroponate ligand in **[Ru]-3** also revealed the formation of  $\{(\kappa^2\text{-aminotroponate})\text{Ru}(\kappa^2\text{-C},N\text{-phenylpyridine})\}$  (**[Ru]-B<sub>3</sub>**) cyclometalated species as major component (90%) in comparison to **[Ru]-A** species (10%).

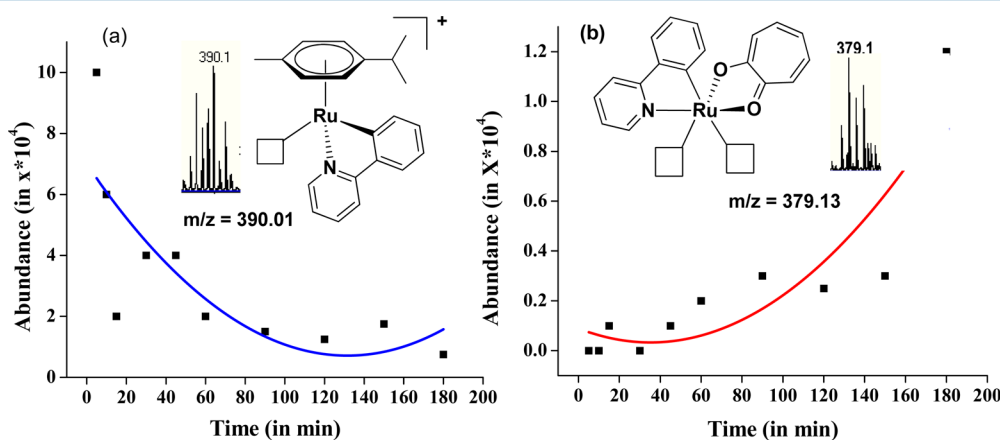


**Figure 7.** Time-dependent study for the formation of (a) species  $\{(\eta^6\text{-arene})\text{Ru}(\kappa^2\text{-C},N\text{-phenylpyridine})\}^+$ , (b) species  $\{(\kappa^2\text{-troponate})\text{Ru}(\kappa^2\text{-C},N\text{-phenylpyridine})\}$ , in substrate-to-catalyst ratio 2:1. (□) Vacant sites.

Therefore, high catalytic efficiency and the detection of troponate/aminotroponate Ru–cyclometalated species **[Ru]-B<sub>1</sub>**–**[Ru]-B<sub>3</sub>** also suggested the key role of the newly identified species in C–H bond arylation reaction. Notably, reaction of **[Ru]-1** with 4-chloroanisole in *S/C* ratio of 5:1 in the presence of  $K_2CO_3$  in water at 100 °C revealed that the **[Ru]-1** is inactive in the presence of aryl chloride. Contrarily, cycloruthenation of 2-phenylpyridine occurred readily with **[Ru]-1** catalyst to generate catalytically active cycloruthenated species **[Ru]-A** and **[Ru]-B** (Figure 7). This further supports that initial C–H bond activation takes place by deprotonation and not by oxidative addition of C–H bond.<sup>34</sup> Literature also revealed that proton abstraction by a carbonate base is energetically favorable process (–13.7 kcal/mol) over hydride abstraction pathway (+28.2 kcal/mol), and during this process base to metal synergy plays a crucial role.<sup>35</sup> The initial carbonate-induced deprotonation of the ortho C–H bond of the phenyl group of 2-phenylpyridine by **[Ru]-1** (as also observed for other complexes **[Ru]-2**–**[Ru]-7**), led to the formation of species **[Ru]-A**, originated by the release of tropolone ligand during the deprotonation process, and **[Ru]-B**, by elimination of  $\eta^6$ -arene ring.<sup>31</sup> Reaction of species **[Ru]-A** with 2.5 equiv of 4-chloroanisole in water at 100 °C resulted in no reaction in the absence of a base ( $K_2CO_3$ ) after 8 h, whereas with 3 equiv of  $K_2CO_3$ , both mono- and diarylated products in 78:22 ratio were observed with 14% conversion. Unfortunately, all our attempts to isolate species **[Ru]-B** failed, presumably, due to the high reactivity of this species. Interestingly, performing the same reaction in methanol formed only **[Ru]-A** species, even after prolonged reaction time, suggesting the crucial role of water in the C–H bond-activation reactions.

Stability of the complexes **[Ru]-1** and **[Ru]-2** in water was monitored by mass-spectral studies over a period of 0 s to one week. Complexes showed high stability in water at room temperature or heating at 100 °C with no sign of decomposition in the absence of base (Figures S5 and S6). These complexes were also found to be stable in water even in the presence of base  $K_2CO_3$  under stirring at room temperature or at 100 °C for 3 d (Figure S7). However, in the presence of  $K_2CO_3$  at 100 °C, release of chloro ligand from complex **[Ru]-1** was observed to be a facile process to form the solvated species  $[(\eta^6\text{-}p\text{-cymene})Ru(\kappa^2\text{-troponate})(CH_3OH)]^+$  (*m/z* 387.1; mass spectra were obtained by diluting the reaction mixture in methanol). Interestingly, complex **[Ru]-2** also showed the release of  $PPh_3$  in the presence of base at 100 °C, but this process was a little sluggish, as prolonged heating for 3 d was required to completely release  $PPh_3$  (Figure S8). Moreover, no sign of the release of arene ligand was observed during mass-spectral studies of the complexes **[Ru]-1** and **[Ru]-2**. Prolonged heating at 100 °C with base for one week resulted in the decomposition of these complexes.

Therefore, we anticipated that under catalytic reaction conditions, in the presence of base and 2-phenylpyridine at 100 °C, release of arene ligand became a more favorable process to generate the catalytically active arene-free ruthenium species **[Ru]-B**. Further, the chelation and strong conjugation effect over seven carbon atoms in the planar ring of tropolone favors the strong interaction of tropolone to ruthenium metal center. As coordination of 2-phenylpyridine earlier to the C–H deprotonation step is crucial, the relative competitive coordination strength of  $\eta^6$ -arene and troponate ligands drive the de-coordination of either troponate ligand or  $\eta^6$ -arene, followed by deprotonation step to form  $[(\eta^6\text{-arene})Ru(\kappa^2\text{-}C,N\text{-phenylpyridine})(sol)]^+$  **[Ru]-A** and

$[(\kappa^2\text{-troponate})Ru(\kappa^2\text{-phenylpyridine})(sol)]_2$  **[Ru]-B<sub>1</sub>**, respectively. This effect is further expected to be responsible for the formation of analogous species **[Ru]-B<sub>3</sub>**, also for aminotroponate complexes **[Ru]-3**,  $[(\kappa^2\text{-isopropylaminotroponate})Ru(\kappa^2\text{-phenylpyridine})(sol)]_2$  (Figure S4).

Support for our experimental results comes from DFT calculations by comparing the relative energies for the formation of species **[Ru]-A**,  $[(\eta^6\text{-arene})Ru(\kappa^2\text{-}C,N\text{-phenylpyridine})(sol)]^+$ , and **[Ru]-B**,  $[(\kappa^2\text{-troponate/aminotroponate})Ru(\kappa^2\text{-phenylpyridine})(sol)]_2$  from complexes **[Ru]-1**, **[Ru]-2**, and **[Ru]-3**. The reaction free energy profile, Figure 8, shows an uphill

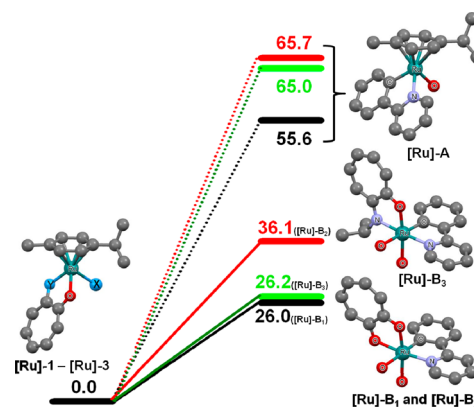
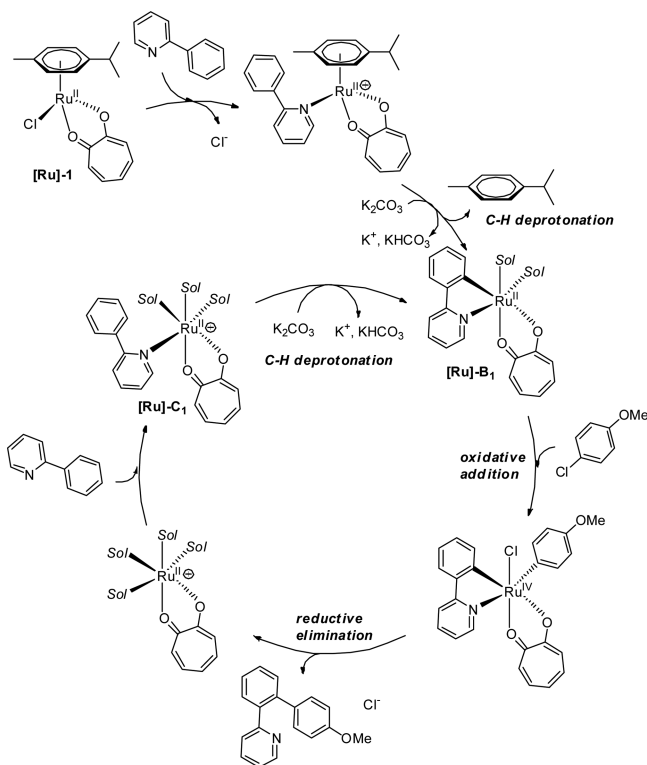


**Figure 8.** Reaction free energy profile for the formation of cycloruthenated species, **[Ru]-A** and **[Ru]-B**, from the reaction of phenylpyridine with troponate/aminotroponate Ru–arene complexes (**[Ru]-1**–**[Ru]-3**).

reaction pathway for the formation of both species **[Ru]-A** and **[Ru]-B** from troponate/aminotroponate Ru–arene complexes. Though the formation of **[Ru]-B** is highly favored over **[Ru]-A** for all the ruthenium complexes, **[Ru]-1** complex showed only marginally higher selectivity for species **[Ru]-B** over **[Ru]-A**, which is in close agreement with our mass-spectral experimental findings. Moreover, binding energy ( $E_B$ ) calculations (Table S5) also showed that *p*-cymene is a better leaving group than tropolone/aminotropolone, and thus the formation of species **[Ru]-B** is favored over species **[Ru]-A**.

On the basis of the mass-spectral identification and well-supported by DFT calculation of new cycloruthenated Ru(II) species, **[Ru]-B** formed as a major component by the release of  $\eta^6$ -arene group during the initial deprotonation step of 2-phenylpyridine, along with the well-established species **[Ru]-A** (minor). Role of species **[Ru]-A** is well-established in C–H bond activation reaction catalyzed by Ru–arene complexes, but our experimental evidence revealed that the formation of species **[Ru]-B** is favored over species **[Ru]-A** for the troponate/aminotroponate ruthenium–arene complexes. Since all the troponate/aminotroponate ruthenium–arene complexes displayed high catalytic activity for C–H bond arylation reaction, species **[Ru]-B** play a key role in the oxidative addition step of C–H bond activation reaction. This observation is also in good agreement with the previous finding by Ackermann et al., that  $RuCl_3(H_2O)_n$  is able to catalyze the C–H arylation in the absence of arene ligands.<sup>36</sup> Hence, a reaction pathway is proposed (shown in Scheme 3) for the C–H bond arylation of 2-phenylpyridine catalyzed by troponate /aminotroponate ruthenium–arene complexes. Notably, troponate/aminotroponate ruthenium–arene complexes are inactive toward direct reaction with aryl chloride, whereas corresponding C–H bond activation of

**Scheme 3. Proposed Reaction Pathway for C–H Bond Arylation of 2-Phenylpyridine Catalyzed by Troponate–Ruthenium(II)–Arene Complex [Ru]-1**



2-phenylpyridine was faster. Given the experimental results for C–H bond arylation of 2-phenylpyridine by several troponate/aminotroponate Ru–arene complexes, it has been established that (i) these complexes are highly efficient catalyst for C–H bond arylation, (ii) increase in steric bulkiness enhances the conversion as well as selectivity toward diarylated product, and (iii) replacing troponate with aminotroponate ligands in ruthenium–arene complexes remarkably enhances the catalytic efficiency and selectivity toward diarylated product.

## CONCLUSION

We successfully synthesized a series of half-sandwiched ruthenium(II) arene complexes with O,O and O,N donor troponate/aminotroponate ligands, and structures of two representative complexes were established by single-crystal X-ray diffraction studies. These synthesized complexes exhibited higher catalytic activity for direct ortho C–H bond arylation of 2-phenylpyridine with 4-chloroanisole at 100 °C in water, without the use of any carboxylate additive, with enhanced selectivity for monoarylated product over diarylated product. In comparison to troponate ruthenium(II)–arene complex [Ru]-1, the selectivity toward monoarylated products is more prominent with aminotroponate ruthenium(II)–arene complexes [Ru]-3 and [Ru]-4. Notably, these complexes are also catalytically active in the presence of carboxylate additive, where selectivity toward diarylated product is favored over monoarylated product with the more bulky carboxylates: pivalate > isobutyrate > propionate > acetate. Extensive mass-spectral studies were performed to identify active key intermediates of the catalyst and to evaluate their role in the C–H bond activation pathway. Our studies showed the formation of a new cycloruthenated species, [Ru]-B, by the release of arene ring from the catalyst, is favored over the

well-established arene–ruthenium cycloruthenated species [Ru]-A. It is worth mentioning here that arene-free ruthenium species, for instance,  $\text{RuCl}_3(\text{H}_2\text{O})_n$ , were also reported to be active for catalytic C–H arylation reactions.<sup>36</sup> These cycloruthenated species were readily generated by carbonate-assisted deprotonation of 2-phenylpyridine by ruthenium complexes. Consistent with the above results, reaction free energies, calculated using DFT calculations, also favored the formation of species [Ru]-B over [Ru]-A. In contrast to the parent ruthenium catalysts, which were inactive with 4-chloroanisole, these cycloruthenated species were found to be active toward oxidative addition of 4-chloroanisole to generate C–H arylated products. On the basis of the experimental evidence, a reaction pathway was proposed showing the key importance of the species [Ru]-B in C–H bond arylation of 2-phenylpyridine. We believe observations marked in the present study using troponate/aminotroponate ruthenium(II)–arene complexes will contribute in enhancing the mechanistic understanding of such catalytic systems in C–H activation reactions and help in development of new and highly active catalytic system. Further investigations in this direction are underway.

## EXPERIMENTAL SECTION

**General Procedure for the Synthesis of Troponone-based Ligands.** Ligands L2 and L3 were synthesized using a literature-reported method with some modifications.<sup>6</sup> 2-Tosyloxypiprone (276 mg, 1.0 mmol), corresponding amine (1.26 mmol), and triethylamine (0.153 g, 1.51 mmol) were dissolved in ethanol (25 mL). The mixture was refluxed for 12 h and then cooled to room temperature. All volatiles were removed under reduced pressure, and the oily residue was taken up in 2 N NaOH (15 mL). The aqueous phase was extracted with  $\text{CH}_2\text{Cl}_2$  (4 × 10 mL). The organic phases were washed with brine (20 mL) and dried with  $\text{Na}_2\text{SO}_4$ . The crude product was purified by column chromatography using silica gel.

**Synthesis of 2-(Isopropylamino)cyclohepta-2,4,6-trienone.** Ligand L2 was prepared by following the above general procedure using 2-tosyloxypiprone (0.276 g, 1.0 mmol), isopropylamine (0.074 g, 1.26 mmol), and triethylamine (0.153 g, 1.51 mmol). Yield: 0.110 g (67.4%).  $^1\text{H}$  NMR (400 MHz,  $\text{CDCl}_3$ ):  $\delta$  (ppm) = 7.18–7.04 (m, 3H), 6.56 (t,  $J$  = 8.0 Hz, 1H), 6.47 (d,  $J$  = 8.0 Hz, 1H), 3.78–3.70 (m, 1H), 1.24 (d,  $J$  = 4.0 Hz, 6H).  $^1\text{H}$  NMR (400 MHz, deuterated dimethyl sulfoxide ( $\text{DMSO}-d_6$ )):  $\delta$  (ppm) = 7.29–7.23 (m, 2H), 6.93 (d,  $J$  = 8.0 Hz, 1H), 6.69–6.61 (m, 2H), 3.91–3.83 (m, 1H), 1.23 (d,  $J$  = 4.0 MHz, 6H).  $^{13}\text{C}$  NMR (100 MHz,  $\text{CDCl}_3$ ):  $\delta$  (ppm) = 176.57, 154.67, 137.18, 136.29, 128.24, 121.83, 108.89, 43.81, 22.02. High-resolution mass spectrometry (HRMS) (electrospray ionization (ESI))  $m/z$  calculated for 2-(isopropylamino)cyclohepta-2,4,6-trienone: 164.1070  $[\text{M} + \text{H}]^+$ , found 164.3049  $[\text{M} + \text{H}]^+$ .

**Synthesis of 2-(Cyclohexylamino)cyclohepta-2,4,6-trienone.** Ligand L3 was prepared by following the above general procedure using 2-tosyloxypiprone (0.276 g, 1.0 mmol), cyclohexylamine (0.125 g, 1.26 mmol), and triethylamine (0.153 g, 1.51 mmol). Yield: 0.140 g (69%).  $^1\text{H}$  NMR (400 MHz,  $\text{CDCl}_3$ ):  $\delta$  (ppm) = 7.17–7.05 (m, 3H), 6.60–6.50 (m, 2H), 3.46–3.41 (m, 1H), 2.02–1.96 (m, 2H), 1.77–1.74 (m, 2H), 1.62–1.59 (m, 1H), 1.37–1.30 (m, 4H), 1.27–1.21 (m, 1H).  $^1\text{H}$  NMR (400 MHz,  $\text{DMSO}-d_6$ ):  $\delta$  (ppm) = 7.28–7.23 (m, 2H), 7.93 (d,  $J$  = 12.0 Hz, 1H), 7.74 (d,  $J$  = 4.0 Hz, 1H), 6.64 (t,  $J$  = 4.0 Hz, 1H), 3.60–3.54 (m, 1H), 1.92–1.89 (m, 2H), 1.70–1.67 (m, 2H), 1.60–1.57 (m, 1H), 1.43–1.29 (m, 4H), 1.23–1.18 (m, 1H).  $^{13}\text{C}$  NMR (100 MHz,  $\text{CDCl}_3$ ):  $\delta$  (ppm) = 176.49, 154.61, 137.12, 136.28, 128.03, 121.78, 108.94, 51.04, 32.07, 25.57, 24.65. HRMS (ESI)  $m/z$  calculated for 2-(cyclohexylamino)cyclohepta-2,4,6-trienone: 204.1389  $[\text{M} + \text{H}]^+$ , found 204.3550  $[\text{M} + \text{H}]^+$ . CCDC deposition number of the ligand L3 is 1431337.

**Procedure for the Synthesis of Ruthenium(II)–Arene Complexes [Ru]-1–[Ru]-8 Containing Troponone and Aminotroponone Ligands.** **Synthesis of  $[(\eta^6\text{-}p\text{-Cymene})\text{Ru}(\kappa^2\text{-O,O-troponone})\text{Cl}]$ .** Troponone

(L1) (0.050 g, 0.41 mmol) and KO<sup>t</sup>Bu (0.046 g, 0.41 mmol) were suspended in methanol (25 mL). The suspension was stirred at room temperature for 3 h then added to  $[(\eta^6\text{-C}_{10}\text{H}_{14})\text{RuCl}_2]_2$  (0.122 g, 0.20 mmol) in suspension. The suspension was stirred at room temperature for 24 h. Solution was evaporated to dryness, and the residue was dissolved in dichloromethane and precipitated by pouring in excess of diethyl ether. Red crystalline solid was obtained. Yield: 0.121 g (77.3%). FTIR (KBr,  $\text{cm}^{-1}$ ): 1221, 1337  $\nu(\text{C}-\text{C})$ , 1508  $\nu(\text{C}=\text{C})$ , 1588.21  $\nu(\text{C}=\text{O})$ . <sup>1</sup>H NMR (400 MHz,  $\text{CDCl}_3$ ):  $\delta$  (ppm) = 7.21 (m, 4H), 6.78 (m, 1H), 5.55 (d, 2H,  $J = 5.2$  Hz), 5.33 (d, 2H,  $J = 4.8$  Hz), 2.89 (sept, 1H), 2.34 (s, 3H), 1.33 (d, 6H,  $J = 6.8$  Hz). <sup>13</sup>C NMR (100 MHz,  $\text{CDCl}_3$ ):  $\delta$  (ppm) = 184.87, 137.80, 127.37, 126.34, 100.48, 96.55, 80.43, 78.89, 31.36, 22.65, 18.89. MS (ESI)  $m/z$  calculated for  $[(\eta^6\text{-C}_{10}\text{H}_{14})\text{Ru}(\text{L1})]^+$  (L1 = tropolone), 357.0  $[\text{M} - \text{Cl}]^+$ , found 357.1  $[\text{M} - \text{Cl}]^+$ . Anal. Calcd: C, 52.04; H, 4.84; O, 8.16. Found: C, 52.08; H, 4.83; O, 8.11%. CCDC deposition number of the complex [Ru]-1 is 1431336.

**Synthesis of  $[(\eta^6\text{-}p\text{-Cymene})\text{Ru}(\kappa^2\text{-}O,O\text{-tropolone})\text{PPh}_3]\text{Cl}$ .**  $[(\eta^6\text{-C}_{10}\text{H}_{14})\text{RuCl}_2(\text{PPh}_3)]$  (0.114 g, 0.20 mmol) and tropolone (L1) (0.026 g, 0.21 mmol) were dissolved in methanol (25 mL), and the solution was refluxed for 12 h. Solution was evaporated to dryness, and the residue was dissolved in dichloromethane and precipitated by diethyl ether. It can be also synthesized by using an alternative method, for which  $[(\eta^6\text{-}p\text{-cymene})\text{RuCl}(\kappa^2\text{-}O,O\text{-tropolone})]$  (0.078 g, 0.20 mmol) and PPh<sub>3</sub> (0.079 g, 0.30 mmol) were suspended in methanol (30 mL), and then the suspension was stirred for 24 h at room temperature. Red microcrystalline solid was obtained. Yield: 0.101 g (77%). <sup>1</sup>H NMR (400 MHz,  $\text{CDCl}_3$ ):  $\delta$  (ppm) = 7.93–7.84 (m, 5H), 7.53–7.44 (m, 10H), 7.43–7.38 (m, 4H), 7.09 (t,  $J = 8.0$  Hz, 1H), 5.26 (b, 2H), 5.06 (b, 2H), 2.92–2.90 (m, 1H), 1.94 (s, 3H), 1.17 (d,  $J = 4.0$  Hz, 6H). MS (ESI)  $m/z$  calculated for  $[(\eta^6\text{-C}_{10}\text{H}_{14})\text{Ru}(\text{L1})\text{PPh}_3]^+$  (L1 = tropolone), 619.1  $[\text{M}^+]$ , found 619.1  $[\text{M}^+]$ . Anal. Calcd: C, 64.26; H, 5.24; O, 4.89. Found: C, 64.19; H, 5.28; O, 4.91%.

**Synthesis of  $[(\eta^6\text{-}p\text{-Cymene})\text{Ru}(\kappa^2\text{-}O,N\text{-}2\text{-}(\text{isopropylamino})\text{-cyclohepta-}2,4,6\text{-trienone})\text{Cl}]$ .** 2-(Isopropylamino)cyclohepta-2,4,6-trienone (L2; 0.163 g, 1.00 mmol) and triethylamine (0.505 g, 5.00 mmol) were suspended in methanol (30 mL), and the suspension was refluxed for 3 h.  $[(\eta^6\text{-C}_{10}\text{H}_{14})\text{RuCl}_2]_2$  (0.275 g, 0.45 mmol) was then added to the above solution, and the solution was refluxed for another 12 h. Solution was filtered and evaporated to dryness, and the residue was dissolved in dichloromethane followed by the precipitation with diethyl ether. Brown crystalline solid was obtained. Yield: 0.320 g (82%). <sup>1</sup>H NMR (400 MHz,  $\text{DMSO-}d_6$ ):  $\delta$  (ppm) = 7.79 (d,  $J = 8.0$  Hz, 1H), 7.40 (d,  $J = 8.0$  Hz, 1H), 6.79 (t,  $J = 8.0$  Hz, 1H), 6.30 (d,  $J = 8.0$  Hz, 1H), 6.10 (t,  $J = 8.0$  Hz, 1H), 5.80 (d,  $J = 4.0$  Hz, 2H), 5.68 (d,  $J = 4$  Hz, 2H), 4.27–4.20 (m, 1H), 2.86–2.78 (sept, 1H), 2.09 (s, 3H), 1.50 (d,  $J = 4.0$  Hz, 3H), 1.40 (d,  $J = 4.0$  Hz, 3H), 1.19 (d,  $J = 4.0$  Hz, 6H). MS (ESI)  $m/z$  calculated for  $[(\eta^6\text{-C}_{10}\text{H}_{14})\text{Ru}(\text{L2})]^+$  (L2 = 2-(isopropylamino)cyclohepta-2,4,6-trienone), 398.1  $[\text{M} - \text{Cl}]^+$ , found 398.1  $[\text{M} - \text{Cl}]^+$ . Anal. Calcd: C, 55.48; H, 6.05; O, 3.70; N, 3.24. Found: C, 55.76; H, 6.15; O, 4.12; N, 3.33%. CCDC deposition number of the complex [Ru]-3 is 1441581.

**Synthesis of  $[(\eta^6\text{-}p\text{-Cymene})\text{Ru}(\kappa^2\text{-}O,N\text{-}2\text{-}(\text{cyclohexylamino})\text{-cyclohepta-}2,4,6\text{-trienone})\text{Cl}]$ .** Complex [Ru]-4 was prepared by following the procedure for the synthesis of complex [Ru]-3, using 2-(cyclohexylamino)cyclohepta-2,4,6-trienone (L3) (0.203 g, 1.00 mmol). Red microcrystalline solid was obtained. Yield: 0.339 g (79%). <sup>1</sup>H NMR (400 MHz,  $\text{DMSO-}d_6$ ):  $\delta$  (ppm) = 6.84–6.68 (m, 3H), 6.31 (d,  $J = 8.0$  Hz, 1H), 6.11 (t,  $J = 8.0$  Hz, 1H), 5.80 (d,  $J = 6.0$  Hz, 2H), 5.76 (d,  $J = 6.0$  Hz, 2H), 3.76–3.66 (m, 1H), 2.81 (sept, 1H), 2.09 (s, 3H), 1.93–1.90 (m, 2H), 1.83–1.77 (m, 3H), 1.68–1.64 (m, 1H), 1.41–1.28 (m, 4H), 1.17 (d,  $J = 4.0$  Hz, 6H). MS (ESI)  $m/z$  calculated for  $[(\eta^6\text{-C}_{10}\text{H}_{14})\text{Ru}(\text{L3})]^+$  (L3 = 2-(cyclohexylamino)cyclohepta-2,4,6-trienone), 438.1  $[\text{M} - \text{Cl}]^+$ , found 438.1  $[\text{M} - \text{Cl}]^+$ . Anal. Calcd: C, 58.40; H, 6.39; O, 3.38; N, 2.96. Found: C, 57.90; H, 5.99; O, 4.01; N, 3.13%.

**Synthesis of  $[(\eta^6\text{-Benzene})\text{Ru}(\kappa^2\text{-}O,O\text{-tropolone})\text{Cl}]$ .**  $[(\eta^6\text{-Benzene})\text{RuCl}_2]_2$  (0.100 g, 0.20 mmol) and tropolone (L1; 0.050 g, 0.41 mmol) were suspended in methanol (25 mL). The suspension was refluxed for 12 h and filtered, and then precipitate was dissolved in

dichloromethane followed by precipitation with excess of diethyl ether. It can be also prepared by following the procedure for the synthesis of complex [Ru]-1. Red microcrystalline solid was obtained. Yield: 0.110 g (82%). FTIR (KBr,  $\text{cm}^{-1}$ ): 1139, 1360  $\nu(\text{C}-\text{C})$ , 1508  $\nu(\text{C}=\text{C})$ , 1588.38  $\nu(\text{C}=\text{O})$ . <sup>1</sup>H NMR (400 MHz,  $\text{CDCl}_3$ ):  $\delta$  (ppm) = 7.23–7.21 (m, 4H), 6.84–6.80 (m, 1H), 5.69 (s, 6H). <sup>13</sup>C NMR (100 MHz,  $\text{CDCl}_3$ ):  $\delta$  (ppm) = 184.29, 137.55, 127.07, 126.41, 80.93. MS (ESI)  $m/z$  calculated for  $[(\eta^6\text{-C}_6\text{H}_6)\text{Ru}(\text{L1})]^+$  (L1 = tropolone), 301.0  $[\text{M} - \text{Cl}]^+$ , found 301.0  $[\text{M} - \text{Cl}]^+$ . Anal. Calcd: C, 46.56; H, 3.30; O, 9.55. Found: C, 46.58; H, 3.17; O, 9.52%.

**Synthesis of  $[(\eta^6\text{-Benzene})\text{Ru}(\kappa^2\text{-}O,O\text{-tropolone})\text{PPh}_3]\text{Cl}$ .** Complex [Ru]-6 was prepared by following the procedure for the synthesis of complex [Ru]-2, using  $[(\eta^6\text{-C}_6\text{H}_6)\text{RuCl}_2(\text{PPh}_3)]$  (0.102 g, 0.20 mmol) and tropolone (L1) (0.026 g, 0.21 mmol) in methanol (25 mL). Red microcrystalline solid was obtained. Yield: 0.102 g (85%). <sup>1</sup>H NMR (400 MHz,  $\text{CDCl}_3$ ):  $\delta$  (ppm) = 7.75–7.72 (m, 5H), 5.43–5.38 (m, 10H), 7.21–7.21 (m, 3H), 5.39 (m, 1H), 5.39 (m, 1H), 5.39 (s, 6H). MS (ESI)  $m/z$  calculated for  $[(\eta^6\text{-C}_6\text{H}_6)\text{Ru}(\text{L1})\text{PPh}_3]^+$  (L1 = tropolone), 563.1  $[\text{M}^+]$ , found 563.1  $[\text{M}^+]$ . Anal. Calcd: C, 62.26; H, 4.38; O, 5.35. Found: C, 62.19; H, 4.13; O, 5.61%.

**Synthesis of  $[(\eta^6\text{-Benzene})\text{Ru}(\kappa^2\text{-}O,N\text{-}2\text{-}(\text{cyclohexylamino})\text{-cyclohepta-}2,4,6\text{-trienone})\text{Cl}]$ .** Complex [Ru]-7 was prepared by following the procedure for the synthesis of complex [Ru]-3, using  $[(\eta^6\text{-C}_6\text{H}_6)\text{RuCl}_2]_2$  (0.225 g, 0.45 mmol). Red microcrystalline solid was obtained. Yield: 0.121 g (80%). <sup>1</sup>H NMR (400 MHz,  $\text{CDCl}_3$ ):  $\delta$  (ppm) = 6.83–6.60 (m, 4H), 6.20 (t,  $J = 8.8$  Hz, 1H), 5.61 (s, 6H), 4.41–4.35 (m, 1H), 1.38 (d,  $J = 6.4$  Hz, 6H). MS (ESI)  $m/z$  calculated for  $[(\eta^6\text{-C}_6\text{H}_6)\text{Ru}(\text{L2})]^+$  (L2 = 2-(isopropylamino)cyclohepta-2,4,6-trienone), 342.0  $[\text{M} - \text{Cl}]^+$ , found 342.0  $[\text{M} - \text{Cl}]^+$ . Anal. Calcd: C, 50.86; H, 5.07; O, 4.29; N, 3.71. Found: C, 50.66; H, 4.87; O, 4.50; N, 3.93%.

**Synthesis of  $[(\eta^6\text{-Benzene})\text{Ru}(\kappa^2\text{-}O,N\text{-}2\text{-}(\text{cyclohexylamino})\text{-cyclohepta-}2,4,6\text{-trienone})\text{Cl}]$ .** Complex [Ru]-8 was prepared by following the procedure for the synthesis of complex [Ru]-7, using 2-(cyclohexylamino)cyclohepta-2,4,6-trienone (L3; 0.203 g, 1.00 mmol). Red microcrystalline solid was obtained. Yield: 0.201 g (53%). MS (ESI)  $m/z$  calculated for  $[(\eta^6\text{-C}_6\text{H}_6)\text{Ru}(\text{L3})]^+$  (L3 = 2-(cyclohexylamino)cyclohepta-2,4,6-trienone), 382.1  $[\text{M} - \text{Cl}]^+$ , found 382.4  $[\text{M} - \text{Cl}]^+$ . Anal. Calcd: C, 54.74; H, 5.32; O, 3.84; N, 3.36. Found: C, 53.13; H, 5.01; O, 2.90; N, 3.10%.

**General Procedure for Catalytic C–H Bond Arylation of Heteroarenes with Aryl Halides.** All the reactions were performed under Ar atmosphere. C–H bond arylation reaction of heteroarene was performed in a two-necked round-bottom flask. Flask was charged with ruthenium catalyst (5 mol %, 0.025 mmol) and  $\text{K}_2\text{CO}_3$  (0.207 g, 1.50 mmol) with distilled water (5 mL). Solution was stirred for 15 min and then added to heteroarene (0.5 mmol) and aryl halide (1.25 mmol). The reaction mixture was degassed with Ar along with the balloon at the top of the fitted condenser. The reaction was continued to stir for 16 h at 100 °C. After completion of reaction time, reaction mixture was cooled to room temperature and extracted with ethyl acetate (3 × 10 mL), and the organic layer was dried over  $\text{Na}_2\text{SO}_4$ . Then extract was washed with 10 mL of saturated brine solution to remove moisture, and the solvent volume was reduced under pressure. The conversion and selectivity of synthesized monoarylated and biarylated products were determined by <sup>1</sup>H NMR. Products were purified and collected from the crude reaction mixture using column chromatography on silica gel with ethyl acetate/*n*-hexane as eluents in 1:99 (v/v) ratio.

## ■ ASSOCIATED CONTENT

### Supporting Information

The Supporting Information is available free of charge on the ACS Publications website at DOI: 10.1021/acs.inorgchem.6b01028.

Materials and instrumentation, tabulated crystal data and refinement details for ligand L3, tabulated bond lengths and bond angles for ligand L3, selected bond lengths and bond angles for complexes [Ru]-1 and [Ru]-3, tabulated cyclic voltammetric data of ruthenium complexes, cyclic

voltammograms, analytical data for catalytic C–H bond arylation reactions, mass-spectral studies of [Ru]-1 with potassium acetate, potassium pivalate, and 2-phenylpyridine, time-dependent mass-spectral study of reaction of [Ru]-1 with 2-phenylpyridine, abundance of [Ru]-A and [Ru]-B with different Ru(II) catalysts, mass-spectral investigation of stability of [Ru]-1 and [Ru]-2 in water, mass spectra, preparation of intermediate species, computational study, optimized structures, tabulated calculated binding energies, additional references, NMR and IR spectra (PDF)

X-ray crystallographic information (CIF)

X-ray crystallographic information (CIF)

X-ray crystallographic information (CIF)

## AUTHOR INFORMATION

### Corresponding Author

\*E-mail: sksingh@iiti.ac.in.

### Notes

The authors declare no competing financial interest.

## ACKNOWLEDGMENTS

Authors thank IIT Indore, CSIR, New Delhi, and SERB (DST), New Delhi, for financial support. SIC, IIT Indore, and NTU, Singapore, are acknowledged for instrumental facilities. A.D.D. thanks CSIR New Delhi research scheme (01(2722)/13/EMR-II) for JRF grant. C.B. thanks MHRD for the fellowship. D.T. thanks UGC New Delhi for SRF grant.

## REFERENCES

- (1) (a) Ackermann, L. *Org. Process Res. Dev.* **2015**, *19*, 260–269. (b) Kumar, P.; Gupta, R. K.; Pandey, D. S. *Chem. Soc. Rev.* **2014**, *43*, 707–733. (c) Li, F.; Collins, J. G.; Keene, F. R. *Chem. Soc. Rev.* **2015**, *44*, 2529–2542. (d) Singh, S. K.; Pandey, D. S. *RSC Adv.* **2014**, *4*, 1819–1840. (e) Crochet, P.; Cadierno, V. *Dalton Trans.* **2014**, *43*, 12447–12462. (f) Gunanathan, C.; Milstein, D. *Chem. Rev.* **2014**, *114*, 12024–12087. (g) Garcia-Álvarez, R.; Díez, J.; Crochet, P.; Cadierno, V. *Organometallics* **2010**, *29*, 3955–3965. (h) Aliende, C.; Perez-Manrique, M. P.; Jalon, F. A.; Manzano, B. R.; Rodriguez, M.; Espino, G. *Organometallics* **2012**, *31*, 6106–6123. (i) Drozdak, R.; Allaert, B.; Ledoux, N.; Dragutan, I.; Dragutan, V.; Verpoort, F. *Coord. Chem. Rev.* **2005**, *249*, 3055–3074.
- (2) (a) Pettinari, R.; Marchetti, F.; Pettinari, C.; Petrini, A.; Scopelliti, R.; Clavel, C. M.; Dyson, P. J. *Inorg. Chem.* **2014**, *53*, 13105–13111. (b) Tyagi, D.; Rai, R. K.; Dwivedi, A. D.; Mobin, S. M.; Singh, S. K. *Inorg. Chem. Front.* **2015**, *2*, 116–124. (c) Gupta, K.; Tyagi, D.; Dwivedi, A. D.; Mobin, S. M.; Singh, S. K. *Green Chem.* **2015**, *17*, 4618–4627. (d) Dwivedi, A. D.; Gupta, K.; Tyagi, D.; Rai, R. K.; Mobin, S. M.; Singh, S. K. *ChemCatChem* **2015**, *7*, 4050–4058. (e) Yamakawa, M.; Ito, H.; Noyori, R. *J. Am. Chem. Soc.* **2000**, *122*, 1466–1478. (f) Davies, D. L.; Fawcett, J.; Garratt, S. A.; Russell, D. A. *Organometallics* **2001**, *20*, 3029–3034. (g) Pelagatti, P.; Carcelli, M.; Calbiani, F.; Cassi, C.; Elviri, L.; Pelizzi, C.; Rizzotti, U.; Rogolino, D. *Organometallics* **2005**, *24*, 5836–5844. (h) Thai, T. T.; Therrien, B.; Süß-Fink, G. *J. Organomet. Chem.* **2009**, *694*, 3973–3981. (i) Phillips, A. D.; Thommes, K.; Scopelliti, R.; Gandolfi, C.; Albrecht, M.; Severin, K.; Schreiber, D. F.; Dyson, P. J. *Organometallics* **2011**, *30*, 6119–6132. (j) Aliende, C.; Pérez-Manrique, M.; Jalón, F. A.; Manzano, B. R.; Rodríguez, A. M.; Espino, G. *Organometallics* **2012**, *31*, 6106–6123. (k) Soldevila-Barreda, J. J.; Bruijninx, P. C. A.; Habtemariam, A.; Clarkson, G. J.; Deeth, R. J.; Sadler, P. J. *Organometallics* **2012**, *31*, 5958–5967. (l) Hohloch, S.; Suntrup, L.; Sarkar, B. *Organometallics* **2013**, *32*, 7376–7385.
- (3) (a) Han Ang, W.; Dyson, P. J. *Eur. J. Inorg. Chem.* **2006**, *2006*, 4008–4018. (b) Süss-Fink, G. *Dalton Trans.* **2010**, *39*, 1673–1688.

(c) Kilpin, K. J.; Cammack, S. M.; Clavel, C. M.; Dyson, P. J. *Dalton Trans.* **2013**, *42*, 2008–2014. (d) Clavel, C. M.; Paunescu, E.; Nowak-Silwinska, P.; Griffioen, A. W.; Scopelliti, R. *J. Med. Chem.* **2015**, *58*, 3356–3365.

(4) Mendiguchia, B. S.; Pucci, D.; Mastropietro, T. F.; Ghedini, M.; Crispini, A. *Dalton Trans.* **2013**, *42*, 6768–6774.

(5) Meyer, N.; Lohnwitz, K.; Zulus, A.; Roesky, P. W.; Dochnahl, M.; Blechert, S. *Organometallics* **2006**, *25*, 3730–3734.

(6) Dochnahl, M.; Lohnwitz, K.; Pissarek, J. W.; Biyikal, M.; Schulz, S. R.; Schon, S.; Meyer, N.; Roesky, P. W.; Blechert, S. *Chem. - Eur. J.* **2007**, *13*, 6654–6666.

(7) Duncan, C.; Biradar, A. V.; Asefa, T. *ACS Catal.* **2011**, *1*, 736–750.

(8) Hicks, F. A.; Jenkins, J. C.; Brookhart, M. *Organometallics* **2003**, *22*, 3533–3545.

(9) Mazzeo, M.; Lamberti, M.; Tuzi, A.; Centore, R.; Pellecchia, C. *Dalton Trans.* **2005**, 3025–3031.

(10) Schutte, M.; Roodt, A.; Visser, H. G. *Inorg. Chem.* **2012**, *51*, 11996–12006.

(11) Yoshida, J.; Kuwahara, K.; Yuge, H. *J. Organomet. Chem.* **2014**, *756*, 19–26.

(12) Mori, A.; Mori, R.; Takemoto, M.; Yamamoto, S.; Kuribayashi, D.; Uno, K.; Kubo, K.; Ujiie, S. *J. Mater. Chem.* **2005**, *15*, 3005–3014.

(13) Dehnen, S.; Bürgstein, M. R.; Roesky, P. W. *J. Chem. Soc., Dalton Trans.* **1998**, 2425–2429.

(14) Becica, J.; Jackson, A. B.; Dougherty, W. G.; Kassel, W. S.; West, N. M. *Dalton Trans.* **2014**, *43*, 8738–8748.

(15) For selected reviews on C–H bond activation: (a) Shilov, A. E.; Shul'pin, G. B. *Chem. Rev.* **1997**, *97*, 2879–2932. (b) Jia, C.; Kitamura, T.; Fujiwara, Y. *Acc. Chem. Res.* **2001**, *34*, 633–639. (c) Labinger, J. A.; Bercaw, J. E. *Nature* **2002**, *417*, 507–514. (d) Ackermann, L.; Vicente, R.; Kapdi, A. R. *Angew. Chem., Int. Ed.* **2009**, *48*, 9792–9826. (e) Mkhaliid, I. A. I.; Barnard, J. H.; Marder, T. B.; Murphy, J. M.; Hartwig, J. F. *Chem. Rev.* **2010**, *110*, 890–931. (f) Gunay, A.; Theopold, K. H. *Chem. Rev.* **2010**, *110*, 1060–1081. (g) Li, B.; Dixneuf, P. H. *Chem. Soc. Rev.* **2013**, *42*, 5744–5767. (h) Ackermann, L. *Acc. Chem. Res.* **2014**, *47*, 281–295. (i) Ackermann, L.; Li, J. *Nat. Chem.* **2015**, *7*, 686–687. (j) Zha, G.-F.; Qin, H.-L.; Kantchev, E. A. B. *RSC Adv.* **2016**, *6*, 30875–30885. (k) Borie, C.; Ackermann, L.; Nechab, M. *Chem. Soc. Rev.* **2016**, *45*, 1368–1386.

(16) (a) Martinez, R.; Simon, M.-O.; Chevalier, R.; Pautigny, C.; Genet, J.-P.; Darses, S. *J. Am. Chem. Soc.* **2009**, *131*, 7887–7895. (b) Ackermann, L.; Barfüßer, S.; Pospesch, J. *Org. Lett.* **2010**, *12*, 724–726. (c) Li, B.; Shi, Z. *Chem. Soc. Rev.* **2012**, *41*, 5588–5598.

(17) (a) Song, G.; Wang, F.; Li, X. *Chem. Soc. Rev.* **2012**, *41*, 3651–3678. (b) Ramirez, T. A.; Zhao, B.; Shi, X. *Chem. Soc. Rev.* **2012**, *41*, 931–942. (c) Louillat, M.; Patureau, F. W. *Chem. Soc. Rev.* **2014**, *43*, 901–910. (d) Mendiola, D. J.; Waterman, R.; Iluc, V. M.; Cundari, T.; Hillhouse, G. L. *Inorg. Chem.* **2014**, *53*, 13227–13238. (e) Gao, B.; Liu, S.; Lan, T.; Huang, H. *Organometallics* **2016**, *35*, 1480–1487.

(18) (a) Matsumoto, K.; Sugiyama, H. *Acc. Chem. Res.* **2002**, *35*, 915–926. (b) Larsen, M. A.; Hartwig, J. F. *J. Am. Chem. Soc.* **2014**, *136*, 4287–4299. (c) Wang, H.; Wang, L.; Shang, J.; Li, X.; Wang, H.; Gui, J.; Lei, A. *Chem. Commun.* **2012**, *48*, 76–78. (d) Shen, C.; Zhang, P.; Sun, Q.; Bai, S.; Hor, T. S. A.; Liu, X. *Chem. Soc. Rev.* **2015**, *44*, 291–314.

(19) (a) Campeau, L. C.; Fagnou, K. *Chem. Commun.* **2006**, 1253–1264. (b) Chen, X.; Engle, K. M.; Wang, D. H.; Yu, J. Q. *Angew. Chem., Int. Ed.* **2009**, *48*, 5094–5115. (c) Lyons, T. W.; Sanford, M. S. *Chem. Rev.* **2010**, *110*, 1147–1169. (d) Beck, E. M.; Gaunt, M. J. *Top. Curr. Chem.* **2009**, *292*, 85–121. (e) Sun, C. L.; Li, B.; Shi, Z. *J. Chem. Commun.* **2010**, *46*, 677–685.

(20) (a) Oi, S.; Sakai, K.; Inoue, Y. *Org. Lett.* **2005**, *7*, 4009–4011. (b) Ackermann, L.; Althammer, A.; Born, R. *Angew. Chem., Int. Ed.* **2006**, *45*, 2619–2622. (c) Oi, S.; Sasamoto, H.; Funayama, R.; Inoue, Y. *Chem. Lett.* **2008**, *37*, 994–995. (d) Yu, B.; Yan, X.; Wang, S.; Tang, N.; Xi, C. *Organometallics* **2010**, *29*, 3222–3226. (e) Paymode, D. J.; Ramana, C. V. *J. Org. Chem.* **2015**, *80*, 11551–11558. (f) Zell, D.;

Warratz, S.; Gelman, D.; Garden, S. J.; Ackermann, L. *Chem. - Eur. J.* **2016**, *22*, 1248–1252.

(21) Arockiam, P.; Poirier, V.; Fischmeister, C.; Bruneau, C.; Dixneuf, P. H. *Green Chem.* **2009**, *11*, 1871–1875.

(22) Singh, K. S.; Dixneuf, P. H. *ChemCatChem* **2013**, *5*, 1313–1316.

(23) Sersen, S.; Kljun, J.; Pozgan, F.; Stefane, B.; Turel, I. *Organometallics* **2013**, *32*, 609–616.

(24) Steyl, G. *Polyhedron* **2007**, *26*, 5324–5330.

(25) Singh, K. S.; Kaminsky, W. J. *Coord. Chem.* **2014**, *67*, 3252–3269.

(26) Singh, K. S.; Svitlyk, V.; Mozharivskiy, Y. *Dalton Trans.* **2011**, *40*, 1020–1023.

(27) Singh, S. K.; Trivedi, M.; Chandra, M.; Sahay, A. N.; Pandey, D. S. *Inorg. Chem.* **2004**, *43*, 8600–8608.

(28) Pittracher, M.; Frisch, U.; Kopacka, H.; Wurst, K.; Müller, T.; Oehninger, L.; Ott, I.; Wuttke, E.; Scheerer, S.; Winter, R. F.; Bildstein, B. *Organometallics* **2014**, *33*, 1630–1643.

(29) Singh, K. S.; Svitlyk, V.; Devi, P.; Mozharivskiy, Y. *Inorg. Chim. Acta* **2009**, *362*, 5252–5258.

(30) (a) Fabre, I.; von Wolff, N.; Le Duc, G.; Ferrer Flegeau, E.; Bruneau, C.; Dixneuf, P. H.; Jutand, A. *Chem. - Eur. J.* **2013**, *19*, 7595–7604. (b) Arockiam, P. B.; Fischmeister, C.; Bruneau, C.; Dixneuf, P. H. *Angew. Chem., Int. Ed.* **2010**, *49*, 6629–6632. (c) Hubrich, J.; Himmler, T.; Rodefeld, L.; Ackermann, L. *ACS Catal.* **2015**, *5*, 4089–4093. (d) Li, J.; Ackermann, L. *Org. Chem. Front.* **2015**, *2*, 1035–1039.

(31) Ferrer Flegeau, E.; Bruneau, C.; Dixneuf, P. H.; Jutand, A. *J. Am. Chem. Soc.* **2011**, *133*, 10161–10170.

(32) Ackermann, L.; Vicente, R.; Potukuchi, H. K.; Pirovano, V. *Org. Lett.* **2010**, *12*, 5032–5035.

(33) (a) Boutadla, Y.; Al-Duaij, O.; Davies, D. L.; Griffith, G. A.; Singh, K. *Organometallics* **2009**, *28*, 433–440. (b) Li, B.; Darcel, C.; Dixneuf, P. H. *ChemCatChem* **2014**, *6*, 127–130.

(34) (a) Ozdemir, I.; Demir, S.; Cetinkaya, B.; Gourlaouen, C.; Maseras, F.; Bruneau, C.; Dixneuf, P. H. *J. Am. Chem. Soc.* **2008**, *130*, 1156–1157. (b) Ackermann, L.; Vicente, R.; Althammer, A. *Org. Lett.* **2008**, *10*, 2299–2302.

(35) Tsurugi, H.; Fujita, S.; Choi, G.; Yamagata, T.; Ito, S.; Miyasaka, H.; Mashima, K. *Organometallics* **2010**, *29*, 4120–4129.

(36) (a) Ackermann, L.; Althammer, A.; Born, R. *Tetrahedron* **2008**, *64*, 6115–6124. (b) Ackermann, L.; Althammer, A.; Born, R. *Synlett* **2007**, *2007*, 2833–2836.